

Digital post-distortion of an ADC analog front-end for gamma spectroscopy measurements

T. Kowalski^{1,2}, G. P. Gibiino³, P. Barmuta^{4,2}, J. Szewiński¹, P. A. Traverso³

¹*National Centre for Nuclear Research, 05-400 Otwock, Poland*

²*Institute of Electronic Systems, Warsaw University of Technology, 00-661 Warsaw, Poland*

³*DEI "G. Marconi", University of Bologna, 40136 Bologna, Italy*

⁴*Dept. Electrical Engineering, KU Leuven, 3000 Leuven, Belgium*

Abstract – This work presents the experimental characterization and digital post-distortion (i.e., digital linearization) of a MHz-range ADC analog front-end for gamma radiation spectroscopy measurements. The front-end was firstly characterized by means of a conventional approach yielding Total Harmonic Distortion (THD) and Effective Number Of Bits (ENOB). Then, it was tested using μ s-range pulsed excitations, which are the typical waveforms encountered in gamma spectroscopy. After applying digital post-distortion, the linearized receiver shows a THD reduced by more than 20 dB, a substantial improvement in ENOB, and a higher accuracy in the acquisition of pulsed waveforms.

I. INTRODUCTION

Gamma radiation spectroscopy, which studies the energy spectra of gamma radiation, is an important tool in nuclear physics, as well as in many other fields like geology [1, 2] and security [3]. Spectroscopy measurements aim at quantifying the energy of gamma particles coming from a targeted source, and at creating a histogram of the measured energies, referred to as the energy spectrum. The energy spectrum, in turn, allows to devise the nuclear composition of a measured radiation source.

A gamma spectrometer consists of an ionizing radiation detector and an electrical signal receiver. The detector converts the radiation energy of the incoming particles into voltage pulses with rise/fall times determined by the detector hardware (e.g., hundreds of nanoseconds), while the pulse amplitude is proportional to the energy of the particle. The most commonly used type of detector consists of a scintillation detector (scintillator) coupled with a Photomultiplier Tube (PMT), while the receivers are nowadays based on electronic digitizers using fast Analog-to-Digital Converters (ADCs) [4]. After the acquisition, the captured voltage pulses must be integrated in time to quantify the energy of the particles, and the accuracy of the retrieved energy spectra heavily depends on the receiver performance.

A block diagram of the typical spectroscopy system is shown in Fig. 1. The ADC analog front-end serves two

purposes. Firstly, it performs signal conditioning, such as attenuation and filtering. In order to maximize the acquisition accuracy, the signal conditioning within the front-end is typically set to match the ADC dynamic range with the amplitudes received from the target radiation. However, when measuring the target sources of radiation such as material samples, higher-energy cosmic radiation might interfere with the measurements, causing voltage pulses with much larger amplitudes. These voltage spikes will typically exceed the ADC full scale, possibly damaging the receiver. Therefore, a second purpose of the front-end is protecting the ADC by means of an analog limiter circuit. Unfortunately, both the signal conditioning and the analog limiter will likely introduce nonlinear distortion, reducing, in practice, the receiver dynamic range.

Digital linearization is an effective approach introduced in the last decades for compensating the nonlinear distortion caused by hardware [5, 6, 7]. The idea consists of the extraction of a suitable mathematical description of the nonlinear dynamic behavior displayed by the device, often derived from the Volterra series representation [7, 8, 9]. The chosen mathematical model is identified through a set of measurements, either using time or frequency domain approaches. Once a suitable direct model of the device is extracted, linearization can be performed by implementing an inverse of the identified model using digital signal processing techniques. Whereas this process is known as digital pre-distortion when linearizing signal generators, transmitters, or power amplifiers [10, 11], it can be implemented as digital post-distortion in the case of receivers [6, 7, 12, 13].

In this work, an analog front-end for gamma spectroscopy measurements has been characterized, both with

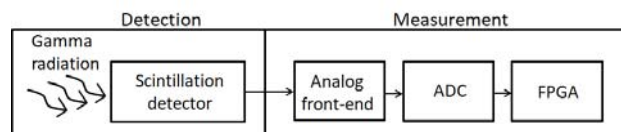


Figure 1. Block diagram of a modern gamma radiation spectroscopy system.

standard methods, using sine wave excitations, as well as using pulsed signals typical of gamma spectroscopy applications. Then, a digital post-distortion approach was successfully implemented, substantially improving the linearity performance of the receiver.

II. EXPERIMENTAL CHARACTERIZATION OF THE ADC FRONT-END

The block diagram of the ADC front-end is shown in Fig. 2. It features a diode, which is aimed at protecting the circuit from nanosecond-range pulses exceeding the full-scale of the ADC, and a signal conditioning stage. The signal conditioning stage is composed by a digital step attenuator for the adjustment of the measurement range, by a fully differential amplifier for signal buffering and single-ended to a differential conversion, and by an anti-aliasing filter.

The characterization of the front-end has been performed by means of the measurement setup shown in Figs. 3 and 4. The output of a 2 GSa/s, 14-bit Arbitrary Wave-

form Generator (AWG, Agilent 81150a) was equally split by means of a power splitter in order to feed two parallel acquisition chains with the same excitation. In the first chain, to be considered as a reference acquisition path, the output of the splitter directly feeds a 100 MHz, 14-bit digitizer board (National Instruments PXI-5122). In the other chain, the input signal is applied to the analog front-end under test. Then, a high-linearity instrumentation amplifier (Tegam 4040) was used to transform the differential output of the front-end into another channel of the same PXI-5122 digitizer board.

Firstly, only the receiver chain comprising the front-end under test was characterized. The test procedure was carried out using sinusoidal tone excitations, and measurement data was then processed according to Standard IEEE 1241 [14]. The considered figures of merit, i.e., the Total Harmonic Distortion (THD) and Effective Number of Bits (ENOB), are reported in Figs. 5 and 6, respectively, for a set of acquired frequencies and amplitudes. As can be seen, a clear dependency on the input signal amplitude was found. While the distortion at -12 dBFS could be satis-

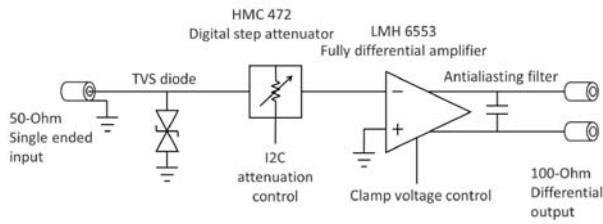


Figure 2. Block diagram of the designed analog front-end under test.

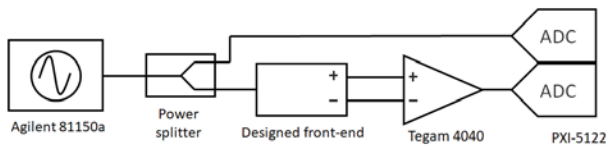


Figure 3. Block diagram of the measurement setup for the characterization of the ADC analog front-end.

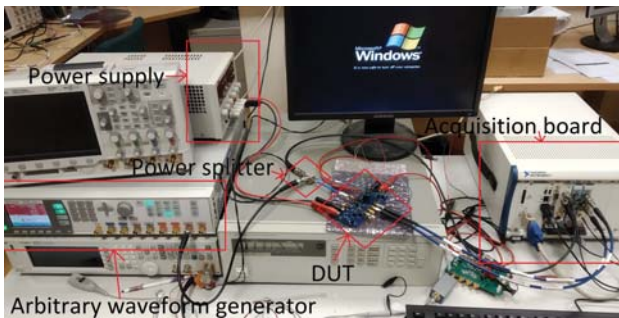


Figure 4. Picture of the measurement setup for the characterization of the ADC analog front-end.

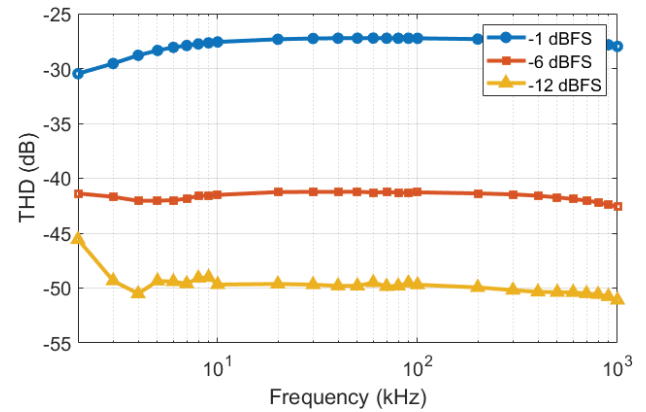


Figure 5. Total harmonic distortion (9 harmonics) of the acquisition chain including the ADC front-end.

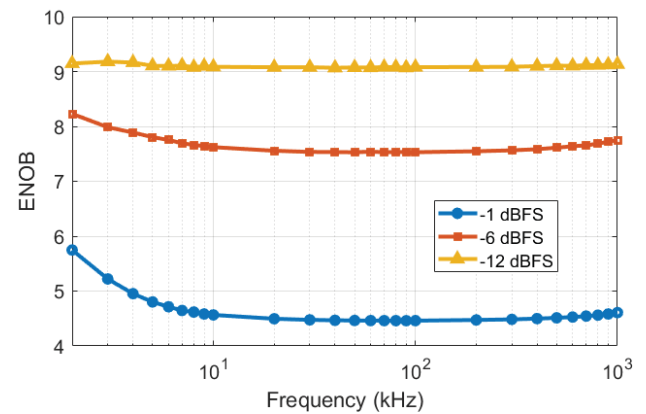


Figure 6. Effective number of bits of the acquisition chain including the ADC front-end.

factory over the measured frequency range, it substantially deteriorates when the excitation approaches the full scale, reporting THD as high as -30 dB and minimum ENOB of around 5 at -1 dBFS. This could be attributed to the non-linear characteristic of the diode, as well as to the low-frequency performance of the switching circuitry inside of the digital step attenuator.

Then, the front-end was tested for application-like spectroscopy measurements. Indeed, in a realistic scenario, the ADC front-end will only receive specific signals, namely exponential pulses of a given duration and different amplitudes. Therefore, an additional characterization was performed employing pulsed excitations modeled from experimental data of an actual scintillator. These pulsed waveforms could be easily generated by programming the AWG in Fig. 1. Then, the impact of the front-end on the pulse shape was quantified by comparing the waveforms distorted by the front-end under test with those acquired through the reference path, which can be considered ideal for the applied excitations.

In particular, 1- μ s and 0.5- μ s pulse-width waveforms were generated with both positive and negative polarities, and sequences of 20 pulses with increasing amplitudes from zero up to the full scale of the ADC front-end were programmed into the AWG. All acquired signals were normalized in amplitude and delay to allow for numerical comparison. Additionally, spectrum equalization was performed to compensate for the baseline wander effect due to the presence of AC-coupling capacitors in the front-end.

In order to characterize the performance of the front-end with respect to the ideal reference, two quantities were used. Firstly, the Normalised Root Mean Square Deviation (NRMSD) between the waveforms acquired from the two channels was calculated. Secondly, as in actual gamma spectroscopy systems, each of the pulses was integrated over time. Then, the NRMSD between the integral values calculated from the actual and reference receivers were obtained, quantifying the deviation that would directly translate into the measured energy spectrum.

Table 1 reports the calculated deviations, while Figs. 7 and 8 show the shape of a single pulse with amplitude equal to the full scale for both acquisition paths. While the negative pulses do not show substantial deviation from the reference, the positive pulses are significantly distorted at full-scale, hinting at the presence of nonlinear dynamic effects.

III. DIGITAL POST-DISTORTION

In order to improve the linearity performance of the receiver under test, a digital post-distortion method was implemented. With post-distortion, the acquired signals are post-processed by inverse modeling of the receiver. In this case, we used a memory polynomial model, which is derived from the Volterra series representation and ne-

glecting the memory cross-terms [10]. Such a mathematical description is well suited for modeling the non-linear dynamic behaviour, and it finds broad use in digital pre-distortion of radio-frequency (RF) power amplifiers. The following memory polynomial formulation was considered [10]:

$$y(n) = \sum_{m=0}^M \sum_{k=1}^K a_{mk} x(n-m) |x(n-m)|^{k-1}, \quad (1)$$

where M is the memory depth and K is the nonlinear order. In theory, a higher order of the model can be

Table 1. Deviations obtained for 0.5- μ s and 1- μ s pulses.

Deviation type	Positive polarity		Negative polarity	
	1 μ s	0.5 μ s	1 μ s	0.5 μ s
NRMSD (%)	5.19	3.34	1.31	1.77
Integral NRMSD (%)	3.44	2.62	1.14	0.88

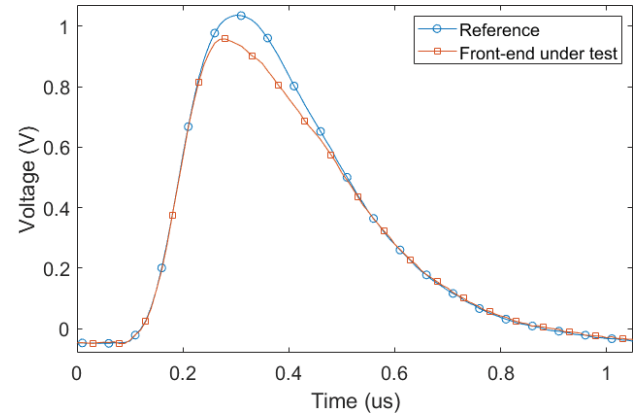


Figure 7. 1- μ s positive pulse with full-scale amplitude, after passing through the two signal acquisition chains.

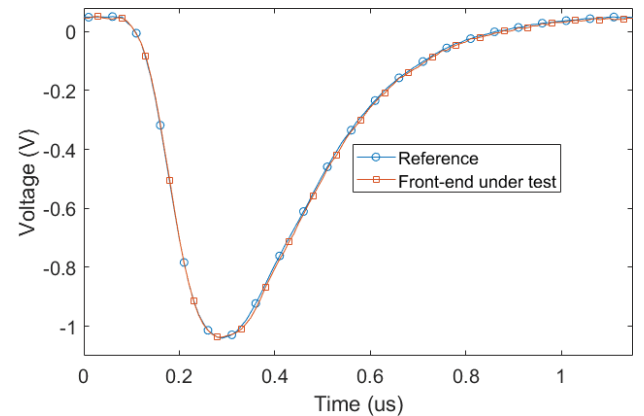


Figure 8. 1- μ s negative pulse with full-scale amplitude after passing through the two signal acquisition chains.

provide better accuracy, as it would include stronger nonlinearities. However, the identification of a large amount of model coefficients can become ill-conditioned, as one should collect an increasingly larger dataset of independent responses. In this research, different tests were carried out by progressively increasing K and M . It was found that increasing the model order beyond $K = 5$ and $M = 3$ did not provide improved prediction capabilities. Then, two particular cases are considered: a static ($M = 0$) polynomial model with $K = 5$, and a memory polynomial model with $K = 5$ and $M = 3$.

Rather than inverting the direct model by means of iterative or nonlinear optimization algorithms, an indirect approach was used for the identification of the inverse model from time-domain measurement data, using the method in [15]. In a first characterization, the inverse models were trained on a dataset composed by acquisitions of sine-wave excitations at 10 kHz, 100 kHz, and 1 MHz. Then, the

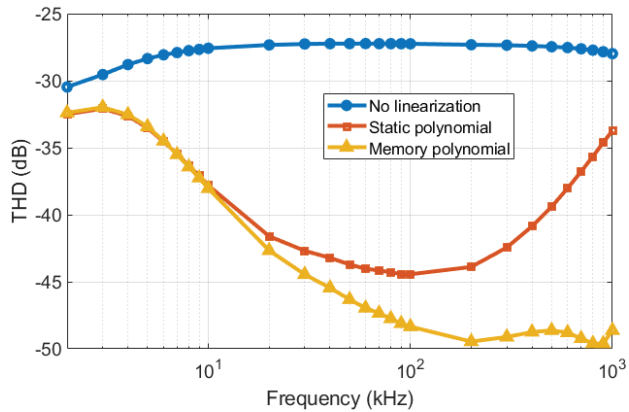


Figure 9. Total harmonic distortion (9 harmonics) of the acquisition chain including the ADC front-end after digital post-distortion, measured at -1 dBFS.

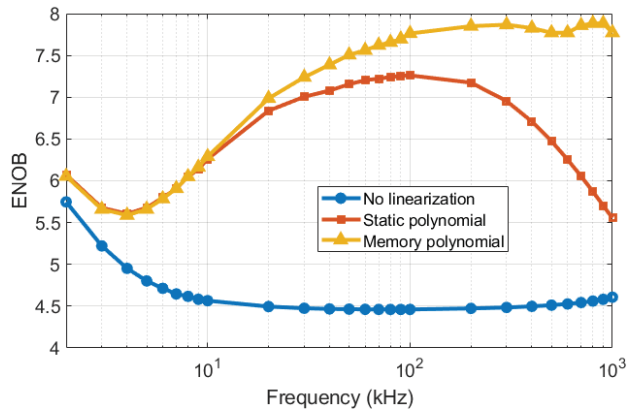


Figure 10. Effective number of bits of the acquisition chain including the ADC front-end after digital post-distortion, measured at -1 dBFS.

whole receiver chain including the analog front-end and the post-distortion processing was characterized according to the IEEE 1241-2010 standard in the frequency range from 1 kHz to 1 MHz. The THD and ENOB calculated after post distortion are respectively plotted in Figs. 9 and 10. In the frequency range from 1 kHz to 1 MHz, an improvement in THD of up to 15 dB was obtained with the static polynomial model, and of up to 20 dB with a memory polynomial model. The corresponding improvement in ENOB is more than 2 bits using the static polynomial model, and more than 3 bits using the memory polynomial model.

Digital post-distortion was also applied for the acquisi-

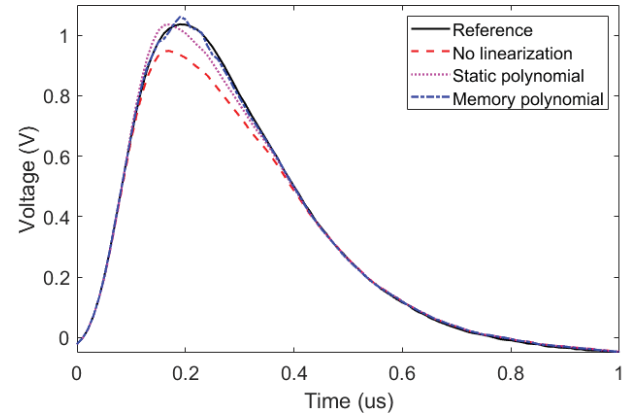


Figure 11. $1\text{-}\mu\text{s}$ positive pulse with full-scale amplitude after digital post-distortion.

Table 2. NRMSD (%) after post-distortion for different pulsed excitations.

Linearization method	Positive polarity		Negative polarity	
	$1\ \mu\text{s}$	$0.5\ \mu\text{s}$	$1\ \mu\text{s}$	$0.5\ \mu\text{s}$
None	5.19	3.34	1.31	1.77
Static polynomial	2.39	1.71	1.23	1.75
Memory polynomial	1.2	1.09	1.0	0.83

Table 3. Integral NRMSD (%) after post-distortion for different pulsed excitations.

Linearization method	Positive polarity		Negative polarity	
	$1\ \mu\text{s}$	$0.5\ \mu\text{s}$	$1\ \mu\text{s}$	$0.5\ \mu\text{s}$
None	3.44	2.62	1.14	0.88
Static polynomial	1.35	1.19	1.03	0.84
Memory polynomial	0.97	1.0	1.03	0.79

tion of pulsed waveforms. In this case, the inverse models were separately trained for 0.5- μ s and 1- μ s pulse lengths, as well as for positive and negative polarities. Fig. 11 shows the pulse shape obtained after post-distortion using different models, and in comparison to the reference channel. Tables 2 and 3 report the values of the deviations from the reference in all tested cases. A significant reduction in the deviations was achieved for positive pulses, which showed the highest distortion. For example, the NRMSD was lowered more than 4 times in the case of 1- μ s pulses. For negative pulses, the post-distortion had less impact, as the behavior of the front-end was found to introduce less distortion. Using an inverse model with memory brings a further improvement only in the case of 1- μ s positive pulses, as the other cases do not show substantial dynamic effects.

IV. CONCLUSION

In this work, a post-distortion methodology has been applied to improve the linearity performance of a ADC analog front-end designed for gamma radiation spectroscopy measurements. The results demonstrate the viability of the approach for both sine-wave excitations as well as for application-like pulsed excitations. Since gamma spectroscopy systems work with pulsed signals having predetermined rise/fall times, inverse models for post-distortion can be accurately trained, providing a considerable improvement of the receiver dynamic range.

REFERENCES

- [1] R. Grasty, R. Shives, Applications of gamma ray spectrometry to mineral exploration and geological mapping, in: Workshop presented at Exploration 97: Fourth Decennial Conference on Mineral Exploration, Vol. 97, 1997.
- [2] F. Ghanbari, Soil sampling and analysis (using high resolution gamma spectroscopy)., Tech. rep., Sandia National Lab.(SNL-NM), Albuquerque, NM (United States) (2007).
- [3] C. L. Fontana, A. Carnera, M. Lunardon, F. Pino, C. Sada, F. Soramel, L. Stevanato, G. Nebbia, C. Carasco, B. Perot, et al., Detection system of the first rapidly relocatable tagged neutron inspection system (rrtnis), developed in the framework of the european h2020 c-bord project, *Physics Procedia* 90 (2017) 279–284.
- [4] G. F. Knoll, Radiation detection and measurement, John Wiley & Sons, 2010.
- [5] D. Hummels, Performance improvement of all-digital wide-bandwidth receivers by linearization of adcs and dacs, *Measurement* 31 (1) (2002) 35–45.
- [6] E. Balestrieri, P. Daponte, S. Rapuano, A state of the art on adc error compensation methods, *IEEE Transactions on Instrumentation and Measurement* 54 (4) (2005) 1388–1394.
- [7] H. Lundin, P. Händel, Look-up tables, dithering and volterra series for adc improvements, in: *Design, Modeling and Testing of Data Converters*, Springer, 2014, pp. 249–275.
- [8] D. Mirri, G. Pasini, P. A. Traverso, F. Filicori, G. Iuculano, A finite-memory discrete-time convolution approach for the nonlinear dynamic modelling of s/h-adc devices, *Computer Standards & Interfaces* 25 (1) (2003) 33–44.
- [9] N. Bjorsell, P. Suchánek, P. Handel, D. Ronnow, Measuring volterra kernels of analog-to-digital converters using a stepped three-tone scan, *IEEE Transactions on Instrumentation and Measurement* 57 (4) (2008) 666–671.
- [10] J. Kim, K. Konstantinou, Digital predistortion of wideband signals based on power amplifier model with memory, *Electronics Letters* 37 (23) (2001) 1417–1418.
- [11] T. Kowalski, B. Dąbek, G. P. Gibiino, S. B. Habib, P. Barmuta, A measurement setup for digital predistortion using direct rf undersampling, in: *2018 22nd International Microwave and Radar Conference (MIKON)*, IEEE, 2018, pp. 438–439.
- [12] K. Shi, A. Redfern, Blind volterra system linearization with applications to post compensation of adc nonlinearities, in: *2012 IEEE International Conference on Acoustics, Speech and Signal Processing (ICASSP)*, IEEE, 2012, pp. 3581–3584.
- [13] Z. Alina, O. Amrani, On digital post-distortion techniques, *IEEE Transactions on Signal Processing* 64 (3) (2015) 603–614.
- [14] S. Tilden, S. Max, J. Blair, F. Alegria, E. Balestrieri, N. Bjorsell, J. Calvin, D. Dallet, P. Daponte, L. De Vito, et al., 1241-2010 IEEE standard for terminology and test methods for analog-to-digital converters.
- [15] C. Eun, E. J. Powers, A new volterra predistorter based on the indirect learning architecture, *IEEE transactions on signal processing* 45 (1) (1997) 223–227.